Numerical Simulation of a Conventional Heat Pipe

Shoeib Mahjoub, and Ali Mahtabroshan

Abstract—The steady incompressible flow has been solved in cylindrical coordinates in both vapour region and wick structure. The governing equations in vapour region are continuity, Navier-Stokes and energy equations. These equations have been solved using SIMPLE algorithm. For study of parameters variation on heat pipe operation, a benchmark has been chosen and the effect of changing one parameter has been analyzed when the others have been fixed.

Keywords—Vapour region; conventional heat pipe; numerical simulation.

I. INTRODUCTION

THE flow in heat pipes vapour region and various researchers have studied porous media[1]. Faghri and Thomas [2] have studied the capillary limit in a concentric annular heat pipe by experimental and analytical method. Also Faghri [3] modelled the vapour flow in concentric annular heat pipe by using a numerical model based on assumption of incompressible flow and was determined the pressure distribution. Faghri and Buchko [4] studied the low-temperature heat pipe with multiple heat sources and the influence of heat source distribution in evaporator section was investigated by numerical analysis and experiments. Tournier and El-Genk [5] studied the transient behaviour of heat pipe by using a numerical model based on finite volume scheme. Zhu and Vafai [6] analysed a three dimensional vapour and liquid flow in an asymmetric flat plate heat pipe. They studied the vapour flow by finite element method using FIDAP code. They also used a non-Darcian model for investigation of liquid flow in porous media. Zhu and Vafai [7] also studied the liquid-vapour coupling and non-Darcian transport in the cylindrical heat pipe. They analysed the flow and pressure distribution in a low-temperature heat pipe. Kim et al [8] used an analytical and experimental investigation on the operational characteristics and thermal optimization of a miniature heat pipe with a grooved wick structure. Nouri-Borujerdi and Layeghi [9] analysed the vapour flow in concentric annular heat pipe using SIMPLE algorithm and staggered grid scheme. They found the pressure distribution for different radial Reynolds numbers. Chan and Faghri [10] analysed the

Sh. Mahjoub is with the Mechanical Engineering Department, Islamic Azad University, Majlessi Branch (corresponding author to provide phone: +98 9131671263; fax: +983115223229; e-mail: Sh_mahjoub@yahoo.com).
A. Mahtabroshan is with the Mechanical Engineering Department, Islamic Azad University, Aligoudarz Branch.

vapour flow and heat conduction through the liquid wick and pipe wall in a heat pipe with single or multiple heat sources. In this paper a numerical model has been used for analysis of parameters, which affects heat pipe operation. The steady state incompressible flow has been solved in cylindrical coordinates in both vapour region and wick structure, using FLUENT software. The Darcy's law has been employed for momentum equation in porous media. The governing equations have been solved using SIMPLE algorithm with collocated grid scheme. The objective of this paper was to study the parameters variation on the operation of a conventional heat pipe.

II. MATHEMATICAL MODEL AND GOVERNING EQUATIONS

A cylindrical heat pipe as shown in Fig. 1 consists of three parts:

1. Evaporator section,
2. Adiabatic (transport) section
3. Condenser section.

Heat applied to evaporator section by an external source is conducted through the pipe wall and wick structure, where it vaporizes the working fluid. The resulting vapour pressure drives the vapour through the adiabatic section to the condenser, where the vapour condenses and releasing its latent heat of vaporization to the provided heat sink. The capillary pressure created by the wick structure, pumps the condensed fluid back to the evaporator. Therefore, the heat pipe can continuously transport the latent heat of vaporization from the evaporator to the condenser section. This process will continue as long as there is sufficient capillary pressure to drive the condensate back to the evaporator.
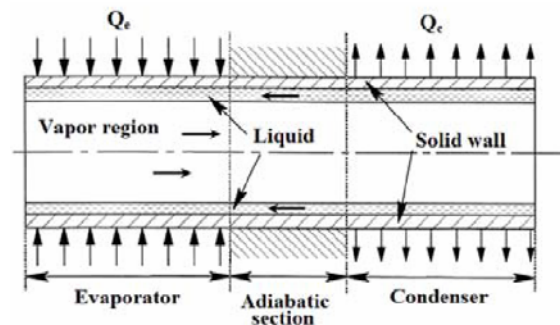

Fig. 1 Schematic of a conventional cylindrical heat pipe

The steady state incompressible laminar flow has been solved in cylindrical coordinates in both vapour region and

World Academy of Science, Engineering and Technology
International Journal of Mechanical and Mechatronics Engineering
Vol:2, No:3, 2008

wick structure. The governing equations in vapour region are continuity, Navier-Stokes and energy equations as following:

$$\frac{\partial u_v}{\partial x} + \frac{\partial v_v}{\partial r} + \frac{v_v}{r} = 0 \tag{1}$$

$$\rho_v\left(u_v\frac{\partial u_v}{\partial x} + v_v\frac{\partial u_v}{\partial r}\right) = \tag{2}$$

$$-\frac{\partial P_v}{\partial x} + \mu_v\left[\frac{4}{3}\frac{\partial^2 u_v}{\partial x^2} + \frac{1}{r}\frac{\partial}{\partial r}\left(r\frac{\partial u_v}{\partial r}\right) + \frac{1}{r}\frac{\partial}{\partial r}\left(r\frac{\partial v_v}{\partial x}\right) - \frac{2}{3}\frac{\partial}{\partial x}\left(\frac{1}{r}\frac{\partial}{\partial r}(r\,v_v)\right)\right]$$

$$\rho_v\left(u_v\frac{\partial v_v}{\partial x} + v_v\frac{\partial v_v}{\partial r}\right) = -\frac{\partial P_v}{\partial r} + \mu_v\left[\frac{\partial^2 v_v}{\partial x^2} + \frac{4}{3r}\frac{\partial}{\partial r}\left(r\frac{\partial v_v}{\partial r}\right) - \frac{4}{3}\frac{v_v}{r^2} + \frac{1}{3}\frac{\partial^2 u_v}{\partial x\partial r}\right] \tag{3}$$

$$\rho_v c_{p,v}\left(u_v\frac{\partial T_v}{\partial x} + v_v\frac{\partial T_v}{\partial r}\right) = \frac{k_v}{r}\left[\frac{\partial}{\partial r}\left(r\frac{\partial T_v}{\partial r}\right) + r\frac{\partial^2 T_v}{\partial x^2}\right] + v_v\frac{\partial p_v}{\partial r} + u_v\frac{\partial p_v}{\partial x} \tag{4}$$

The boundary conditions for vapour region are as following. The radial velocities at liquid-vapour interface [9]:

$$\begin{cases} v_e = +\dfrac{\dot{Q}_e}{2\pi R_{Int}L_e\rho_v h_{fg}} \\[2mm] v_a = 0 \\[2mm] v_c = -\dfrac{\dot{Q}_c}{2\pi R_{Int}L_c\rho_v h_{fg}} \end{cases} \tag{5}$$

The temperature at the vapour-liquid interface of the evaporator and condenser is calculated approximately using Clausius-Clapeyron equation [9]:

$$T_{int} = \frac{1}{\dfrac{1}{T_{v,sat}} - \dfrac{R}{h_{fg}}\ln\dfrac{P_v}{P_{v,sat}}} \tag{6}$$

The boundary conditions at both pipe ends are:

$$v = u = 0 \qquad \frac{\partial T_v}{\partial x} = 0 \tag{7}$$

At pipe centreline the symmetry boundary conditions are:

$$v = 0, \quad \frac{\partial u}{\partial r} = 0 \ \& \ \frac{\partial T}{\partial r} = 0 \tag{8}$$

The governing equations in wick structure are as following. The Darcy's law has been employed for momentum equation in porous media:

$$\rho_l\left(u_l\frac{\partial u_l}{\partial x} + v_l\frac{\partial u_l}{\partial r}\right) = -\frac{\partial P_l}{\partial x} + \mu_l\left[\frac{1}{r}\frac{\partial}{\partial r}\left(r\frac{\partial u_l}{\partial r}\right) + \frac{\partial^2 u_l}{\partial x^2}\right] - \frac{\mu_l\varepsilon_x u_l}{K_x} \tag{9}$$

$$\rho_l\left(u_l\frac{\partial v_l}{\partial x} + v_l\frac{\partial v_l}{\partial r}\right) = -\frac{\partial P_l}{\partial r} + \mu_l\left[\frac{1}{r}\frac{\partial}{\partial r}\left(r\frac{\partial v_l}{\partial r}\right) + \frac{\partial^2 v_l}{\partial x^2}\right] - \frac{\mu_l\varepsilon_r u_l}{K_r} \tag{10}$$

$$\rho_l c_{p,l}\left(u_l\frac{\partial T_l}{\partial x} + v_l\frac{\partial T_l}{\partial r}\right) = \frac{k_{eff}}{\varepsilon}\left[\frac{1}{r}\frac{\partial}{\partial r}\left(r\frac{\partial T_l}{\partial r}\right) + \frac{\partial^2 T_l}{\partial x^2}\right] + S \tag{11}$$

For homogenous isotropic wicks, the porosity and permeability are the same in all directions, so

$$\varepsilon_r = \varepsilon_x = \varepsilon \qquad K_r = K_x = K \tag{12}$$

The effective thermal conductivity of wick structure, is calculated from equation for screen wire mesh, [1]

$$k_{eff} = \frac{k_l\left[(k_l+k_s) - (1-\varepsilon)(k_l-k_s)\right]}{\left[(k_l+k_s) + (1-\varepsilon)(k_l-k_s)\right]} \tag{13}$$

Since the phase change phenomena was not included in current model, for modeling latent heat of vaporization a heat

sink was employed in evaporator section and a heat source was used in condenser section. The values of these terms are:

$$\begin{cases} S_e = -\dfrac{\dot{Q}_e}{\pi((R_{Int}+t)^2 - R_{Int}^2)L_e} \\[2mm] S_a = 0 \\[2mm] S_c = +\dfrac{\dot{Q}_c}{\pi((R_{Int}+t)^2 - R_{Int}^2)L_c} \end{cases} \tag{14}$$

The boundary conditions at both pipe ends are:

$$v = u = 0 \qquad \frac{\partial T_l}{\partial x} = 0 \tag{15}$$

The radial blowing and suction velocities at liquid-vapour interface [9]:

$$v_e = -\frac{\dot{Q}_e}{2\pi R_{Int}L_e\rho_v h_{fg}} \qquad v_a = 0 \qquad v_c = +\frac{\dot{Q}_c}{2\pi R_{Int}L_c\rho_v h_{fg}} \tag{16}$$

At heat pipe wall the equation of thermal conduction was used in cylindrical coordinates:

$$k_{Solid}\left[\frac{1}{r}\frac{\partial}{\partial r}\left(r\frac{\partial T_{Solid}}{\partial r}\right) + \frac{\partial^2 T_{Solid}}{\partial x^2}\right] = 0 \tag{17}$$

The boundary conditions in this region are as following:
At wall-liquid interface:

$$k_{eff}\frac{\partial T_l}{\partial r} = k_{Solid}\frac{\partial T_{Solid}}{\partial r} \tag{18}$$

At both ends of heat pipe:

$$\frac{\partial T_{Solid}}{\partial x} = 0 \tag{19}$$

At external surface of heat pipe:

$$\begin{cases} \dfrac{\partial T_{Solid}}{\partial r} = +\dfrac{\dot{Q}_e}{2\pi R_{Out}L_e} & Condensor \\[2mm] \dfrac{\partial T_{Solid}}{\partial r} = 0 & Adiabatic \\[2mm] \dfrac{\partial T_{Solid}}{\partial r} = -\dfrac{\dot{Q}_c}{2\pi R_{Out}L_c} & Evaporator \end{cases} \tag{20}$$

III. METHOD OF SOLUTION

The governing equations are discredited using a finite volume approach and equations were solved using SIMPLE algorithm with collocated grid scheme. The physical domain of problem was separated into 2 regions as follows.
1. vapour region
2. wick structure and pipe wall
The numerical analysis was performed in both separated region. The solution procedure is as follows.
1. Continuity and momentum equation are solved in vapour region with mentioned boundary conditions to find the pressure distribution.
2. Equation (6) has been used to find temperature boundary condition at the vapour-liquid interface.
3. All of equations have been solved in vapour region.
4. The mentioned equations with related boundary conditions have been solved in wick structure and pipe wall simultaneously.

World Academy of Science, Engineering and Technology
International Journal of Mechanical and Mechatronics Engineering
Vol:2, No:3, 2008

IV. MODEL VERIFICATION

For verification of current model, the results of pressure distributions for an annular concentric heat pipe which specification are in Table I have been compared with other results. As shown in Fig. 2 and Fig. 3, the result has good agreement.

V. CHECKING FOR GRID INDEPENDENCY

The domain was discredited with structural homogenous meshes. The equations of porous media have been solved with various numbers of meshes and as shown in Fig. 4, 41839 nodes were sufficient to achieve results that were independent to mesh structure.

TABLE I
SPECIFICATIONS OF ANNULAR CONCENTRIC HEAT PIPE USED FOR MODEL
VERIFICATION, [3] AND [9]

Heat pipe wall material	Copper
Ratio of internal to external diameter	0.2 and 0.8
Heat pipe length	1000mm
Evaporator length	200mm
Condenser Length	200mm
Working fluid specifications	$h_{fg} = 2251.2 \frac{kJ}{kg}$ $C_p = 2.034 \frac{kJ}{kgK}$ $\rho = 0.5974 \frac{kg}{m^3}$ $\mu = 121.00e-7\,Pa.\sec$ $k = 0.0248 \frac{W}{m.K}$ $T_{sat} = 373.15\,K$
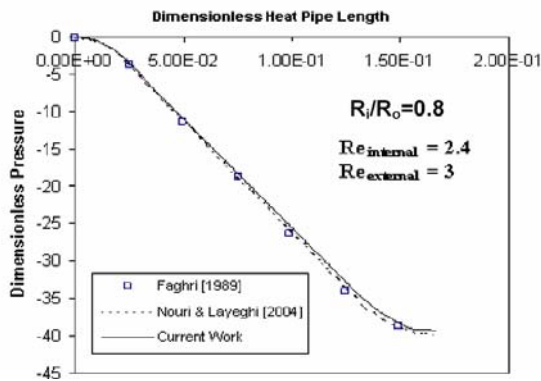
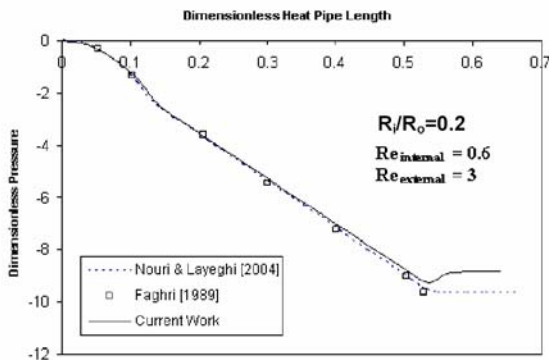Fig. 2 Comparing current model with available numerical data

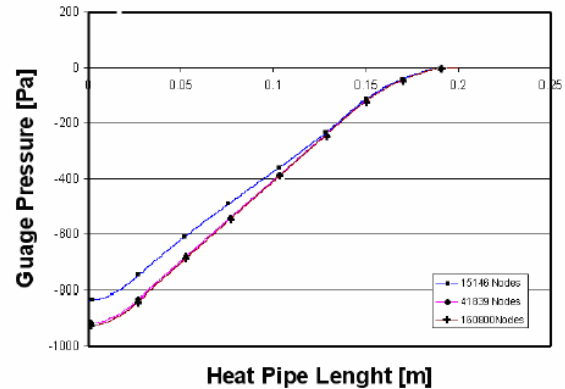Fig. 3 Comparing current model with available numerical data

Fig. 4 Checking for grid independency

VI. STUDY OF PARAMETERS VARIATIONS

For study of parameters variation on heat pipe operation, a benchmark has been chosen and the effect of changing one parameter has been analysed when the others have been fixed. The benchmark specification is given in Table II.

TABLE II
SPECIFICATIONS OF BENCHMARK HEAT PIPE

Heat pipe container material	Copper
Wall thickness	0.15mm
Type of porous media	Screen SST 400
Wick thickness	0.75mm
Porosity	0.733
Outer diameter	8.9mm
Heat pipe length	200mm
Evaporator length	25mm
Condenser length	60mm
Working fluid	Distilled water
Saturated Temperature	323 K

A. Thermal Conductivity of Heat Pipe Wall

Here the effect of thermal conductivity of heat pipe wall to outer surface temperature distribution and thermal resistance of system was studied. As Fig. 5 Shows with increasing of thermal conductivity of heat pipe wall, the maximum temperature of outer surface decreases. Also it is seen from Fig. 6 that with increasing wall thermal conductivity, the thermal resistance of system decreases.
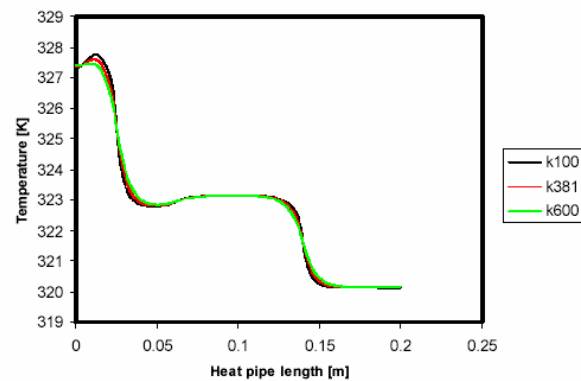

Fig. 5 Wall temperature distribution with reference to Variation of wall thermal conductivity

World Academy of Science, Engineering and Technology
International Journal of Mechanical and Mechatronics Engineering
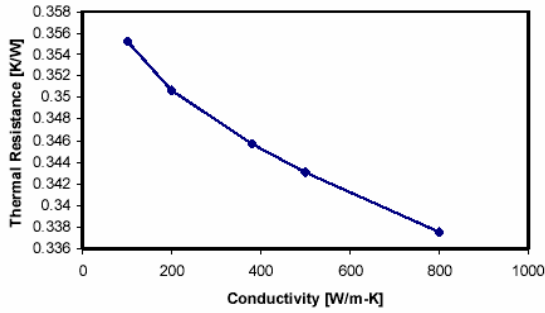Vol:2, No:3, 2008

Fig. 6 Thermal resistance of heat pipe with reference to variation of wall thermal conductivity

B. Wick Porosity

Here the effect of wick porosity to the heat pipe behaviour was studied. With increasing the porosity, the effective thermal conductivity of wick structure decreases, so the temperature differences in evaporator and condenser increases. (Fig. 7). Also with increasing the porosity, the pressure drops in wick structure decreases and the thermal resistance of system increases. (Fig. 8)
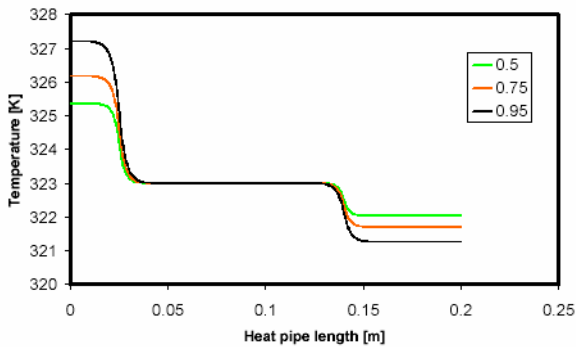
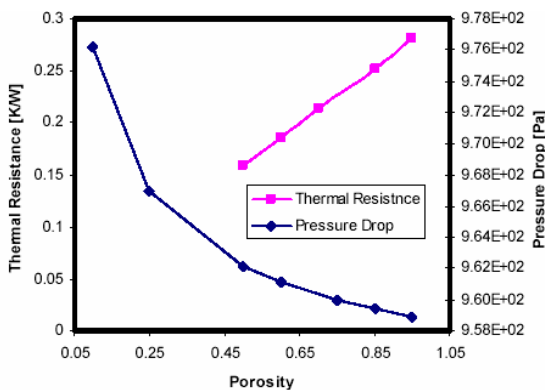Fig. 7 Heat pipe wall temperature with reference to variation of wick porosity

Fig. 8 Pressure drop in liquid region and thermal resistance of heat pipe with reference to variation of wick porosity

C. Transmitting Heat Power

With different values of internal heat power in evaporator, the behaviour of heat pipe was studied. As shown in Fig. (9), with increasing the transmitting heat the temperature difference in evaporator and condenser section increases. Also

with increasing transmitting heat power, the pressure drop in liquid region increases since the flow rate of liquid increases (Fig. 10). Fig. 11 shows the thermal resistance variations and pressure drop with reference to transmitting heat power, it was seen that for moderate transmitting heat power the thermal resistance of system is approximately constant.
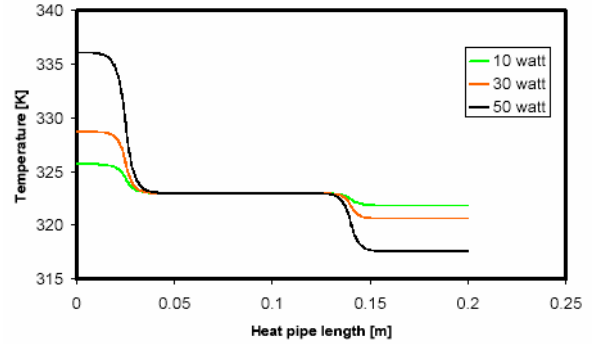

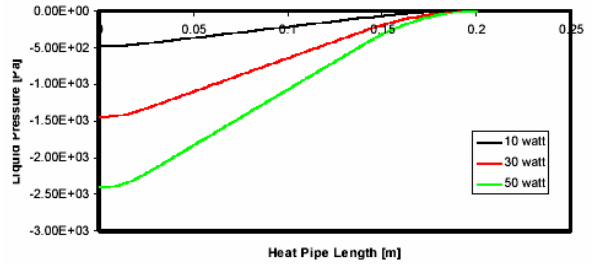Fig. 9 Heat pipe wall temperature with reference to variation of transmitting heat power

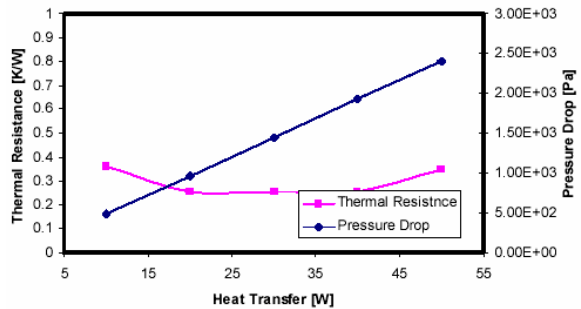Fig. 10 Liquid pressure distribution with reference to variation of transmitting heat power

Fig. 11 Pressure drop in liquid region and thermal resistance of heat pipe with reference to variation of transmitting heat power

D. Heat Pipe Radius

Here the effect of heat pipe radius to outer surface temperature distribution, pressure drop and thermal resistance of system was studied. As shown in Fig. 12 with increasing heat pipe radius, the temperature difference in evaporator and condenser section decreases. For the reason it can be said that with increasing heat pipe radius the heat transfer area increases. Also as shown in Fig. 13, with increasing heat pipe radius, the flow area increases and it causes, decreasing in pressure drop in liquid region. The variation of thermal

World Academy of Science, Engineering and Technology
International Journal of Mechanical and Mechatronics Engineering
Vol:2, No:3, 2008

resistance with respect to heat pipe radius was shown in Fig. 14.
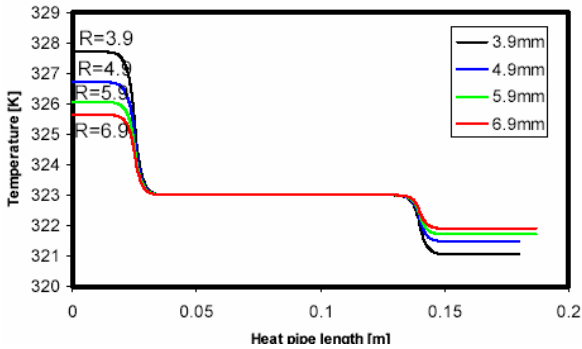

Fig. 12 Heat pipe wall temperature distribution with respect to variation of radius
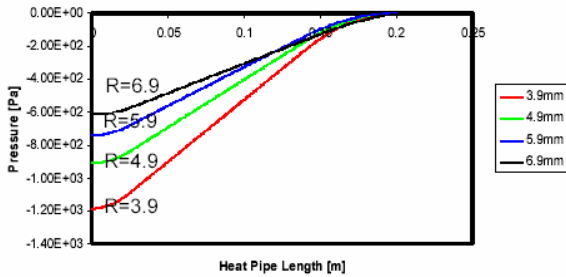

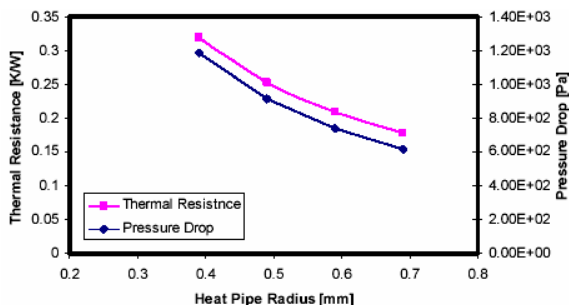Fig. 13 Pressure distribution in liquid region with respect to Variation of radius

Fig. 14 Pressure drop in liquid region and thermal resistance of heat pipe with reference to variation of radius

E. Heat Pipe Length

The last parameter that the effect of its variation on heat pipe behaviour was studied is the length of heat pipe. As shown in Fig. 15 with increasing heat pipe length, the temperature difference between evaporator and condenser is constant so the thermal resistance of heat pipe remains constant. The pressure distribution in liquid region was shown in Fig. 16, as it seen with increasing heat pipe length, the pressure drop increases too. For the reason it can be said that with increasing heat pipe length, the liquid path from condenser to evaporator increases. The variation of thermal resistance and liquid pressure drop with respect to heat pipe length was shown in Fig. 17.
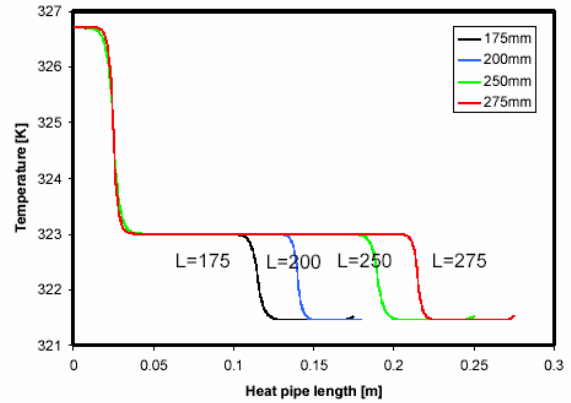

Fig. 15 Heat pipe wall temperature distribution with respect to variation of length
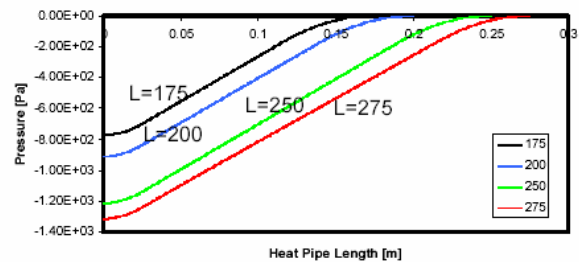

Fig. 16 Pressure distribution in liquid region with respect to Variation of heat pipe length
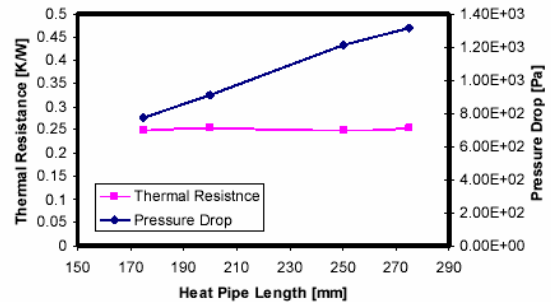

Fig. 17 Pressure drop in liquid region and thermal resistance of heat pipe with reference to variation of length

VII. CONCLUSION

It has been shown that steady state two-dimensional heat transfer and flow equations in both vapour region and porous media can be simulated using this numerical model with accuracy. For design of a heat pipe for a special purpose it is possible to study parameter variation and their effect on system behaviour. The governing equations have been solved using SIMPLE algorithm with collocated grid scheme. This model has been verified with available numerical data and has shown good agreement. The results shows that, thermal resistance of a conventional cylindrical heat pipe, grows with increasing wick porosity, and decreases with increasing of wall thermal conductivity and heat pipe radius.

REFERENCES

[1]   Amir Faghri, Heat Pipe Science and Technology, Taylor & Francis Publishing, 1995.

World Academy of Science, Engineering and Technology
International Journal of Mechanical and Mechatronics Engineering
Vol:2, No:3, 2008

[2] A. Faghri and S. Thomas, "Performance Characteristics of a Concentric Annular Heat Pipe: Part I- Experimental Prediction and Analysis of the Capillary Limit," Transaction of ASME: Journal of Heat Transfer, Vol. 111, pp. 844-850, 1989.

[3] A. Faghri, "Performance Characteristics of a Concentric Annular Heat Pipe: Part II- Vapour Flow Analysis," Transaction of ASME: Journal of Heat Transfer, Vol. 111, pp. 851-857, 1989.

[4] A. Faghri and M. Buchko "Experimental and Numerical Analysis of Low-Temperature Heat Pipes with Multiple Heat Sources," Transaction of ASME: Journal of Heat Transfer, Vol. 113, pp. 728-734, 1991.

[5] J. M. Tournier and M. S. El-Genk, "A Heat Pipe Transient Analysis Model," Int. J. Heat Mass Transfer, Vol. 37, No. 5, pp. 753-762, 1994.

[6] N. Zhu and K. Vafai, "Vapour and Liquid Flow in an Asymmetric Flat Plate Heat Pipe: A Three Dimensional Analytical and Numerical Investigation," Int. J. Heat Mass Transfer, Vol. 41, No. 1, pp. 159-174, 1998.

[7] N. Zhu and K. Vafai, "Analysis of Cylindrical Heat Pipe Incorporating the Effect of Liquid-Vapour Coupling and Non-Darcian Transport-A Closed form Solution," Int. J. Heat Mass Transfer, Vol. 42, pp. 3405-3418, 1999.

[8] S. J. Kim, J. K. Seo and K. H. Do, "Analytical and Experimental Investigation on the Operational Characteristics and Thermal Optimization of a Miniature Heat Pipe with a Grooved Wick Structure," Int. J. Heat Mass Transfer, Vol. 46, pp. 2051-2063, 2003.

[9] A. Nouri-Borujerdi and M. Layeghi, "Numerical Analysis of Vapour Flow in Concentric Annular Heat Pipes," Transaction of ASME: Journal of Heat Transfer, Vol. 126, pp. 442-448, 2004.

[10] M. M. Chan and A. Faghri, "An Analysis of The Vapour Flow and Heat Conduction Through The Liquid Wick and Pipe Wall in a Heat Pipe With Single or Multiple Heat Sources," Int. J. Heat Mass Transfer, Vol. 33, No. 9, pp. 194, 1995.

Sh. Mahjoub received his MSc degree in Mechanic/Thermo-Fluid from Sharif University of Technology. His current research interest includes Fluid mechanic and CFD.

A. Mahtabroshan received his MSc degree in Mechanic/Thermo-Fluid from Sharif University of Technology. His current research interest includes Fluid mechanic and CFD.